Letter

Depinning transition of self-propelled particles

Arthur V. Straube [*] and Felix Höfling

Zuse Institute Berlin, Takustraße 7, 14195 Berlin, Germany

and Department of Mathematics and Computer Science, Freie Universität Berlin, Arnimallee 6, 14195 Berlin, Germany

(Received 15 June 2023; revised 10 April 2024; accepted 5 November 2024; published 5 December 2024)

For self-propelled particles in a corrugated potential landscape, we describe a discontinuous change of the classical depinning transition and a host of unique behaviors sensitive to the persistence of the propulsion direction. Exact and semianalytic results for active Brownian particles corroborate a creep regime with a superexponentially suppressed drift velocity upon lowering the force towards the threshold value. This unusual nonlinear response emerges from the competition of two critical scaling laws with exponents of 1/2 for rapidly reorienting particles and $d/2$ for particles with a persistent orientation; the latter case depends on the dimensionality d of rotational motion and also includes run-and-tumble particles. Additionally, different giant diffusion phenomena occur in the two regimes. Our findings extend to random dynamics with bounded noise near a saddle-node bifurcation and have potential applications in various nonequilibrium problems, including arrested active matter and cell migration.

DOI: 10.1103/PhysRevE.110.L062601

Introduction. A depinning transition occurs when a physical system is driven out of an immobile state by an external force f such that, upon increasing the force above a critical value f_c, the system depins and starts to drift with a velocity v_D [1–3]. Approaching the transition from above, this response scales as $v_D \sim (f - f_c)^\beta$, with a universal exponent β. The phenomenon appears in a variety of contexts: it governs the onset of motion of fronts [4–6], contact lines [7], and domain walls [8–10], as well as vortices in superconductors [11–13] and magnetic skyrmions [14]. The depinning transition is fundamental for the phenomena of sliding friction and superlubricity [15–19], synchronization [20], and locking [21–26]. Colloidal systems have provided insight into the depinning transition of individual particles [27–30], monolayers [31–34], and in glasses [35–37].

Unlike passive matter, active particles—motile microorganisms, artificial microswimmers, and active colloids—propel themselves and perform a persistent motion, with direction randomized over time [38–42]. Experimental research in this field is fueled by the vision of microrobots performing specific transport tasks [43–45]; such particles move through structured channels, blood vessels, or surmount geometric constrictions [46]. More fundamentally, the inherently nonequilibrium nature of self-propulsion leads to a complex interplay with a patterned substrate [42,47–52], which changes the macroscopic transport and yields, e.g., directionality [53], negative mobility [54,55], or superdiffusion [56]. Self-propulsion also produces counterintuitive behaviors in Kramers' escape over high barriers [57–60]. An open issue is the impact of active motion on the depinning transition, i.e., the nonlinear response to external driving, which has potential relevance to a range of applications, including cell migration [61–64].

In this Letter, by combining exact theory with a semianalytical treatment and stochastic simulations, we show that self-propulsion gives rise to a hitherto undescribed kind of depinning transition. The phenomenology is found to be sensitive to the persistence and the dimensionality d of rotational motion. Our findings encompass two scaling regimes with exponents $\beta = 1/2$ and $\beta' = d/2$, an unusual creep regime with superexponentially suppressed drift, a splitting of the force threshold into two singular points, and in between them different unbounded enhancements of the dispersion.

Specifically, we consider the paradigm of the active Brownian particle (ABP) confined to a periodic potential energy landscape $U(\boldsymbol{r})$ and subjected to an external force $\boldsymbol{f}$ [Fig. 1(a)]. The ABP's position $\boldsymbol{r}$ and the orientation $\boldsymbol{u}$ satisfy the Itō–Langevin equations [65,66]:

$$\dot{\boldsymbol{r}}(t) = \mu_0[\boldsymbol{f} - \nabla U(\boldsymbol{r}(t))] + v_A \boldsymbol{u}(t) + \boldsymbol{\xi}(t)\,, \tag{1a}$$

$$\dot{\boldsymbol{u}}(t) = \boldsymbol{\omega}(t) \times \boldsymbol{u}(t) - \tau_R^{-1} \boldsymbol{u}(t)\,, \tag{1b}$$

where $v_A \geqslant 0$ is the propulsion strength and μ_0 is the mobility of the free particle. The random linear and angular velocities, $\boldsymbol{\xi}$ and $\boldsymbol{\omega}$, respectively, are unbiased Gaussian white noise processes with covariances $\langle \boldsymbol{\xi}(t) \otimes \boldsymbol{\xi}(t') \rangle = 2D_0 \mathbb{1}\, \delta(t - t')$ and $\langle \boldsymbol{\omega}(t) \otimes \boldsymbol{\omega}(t') \rangle = 2D_R \mathbb{1} \delta(t - t')$ for the translational and rotational diffusion constants D_0 and D_R, respectively, and τ_R is the persistence time of the orientation. With $\tau_R^{-1} = (d-1)D_R$, Eq. (1b) describes free diffusion of $\boldsymbol{u}(t)$ on the unit circle ($d = 2$) or unit sphere ($d = 3$) [66]. In particular, the process $\boldsymbol{u}(t)$ is isotropic and non-Gaussian with $|\boldsymbol{u}(t)| = 1$ and $\langle \boldsymbol{u}(t) \cdot \boldsymbol{u}(t') \rangle = \exp(-|t - t'|/\tau_R)$. We will focus on the case $d = 3$, which is relevant for colloidal particles [48,67–69]. Results are also provided for $d = 2$ and large τ_R; this setup coincides with the depinning problem of run-and-tumble particles (RTPs) mimicking the motion of bacteria such as *E. coli* [70,71].

[*]Contact author: straube@zib.de

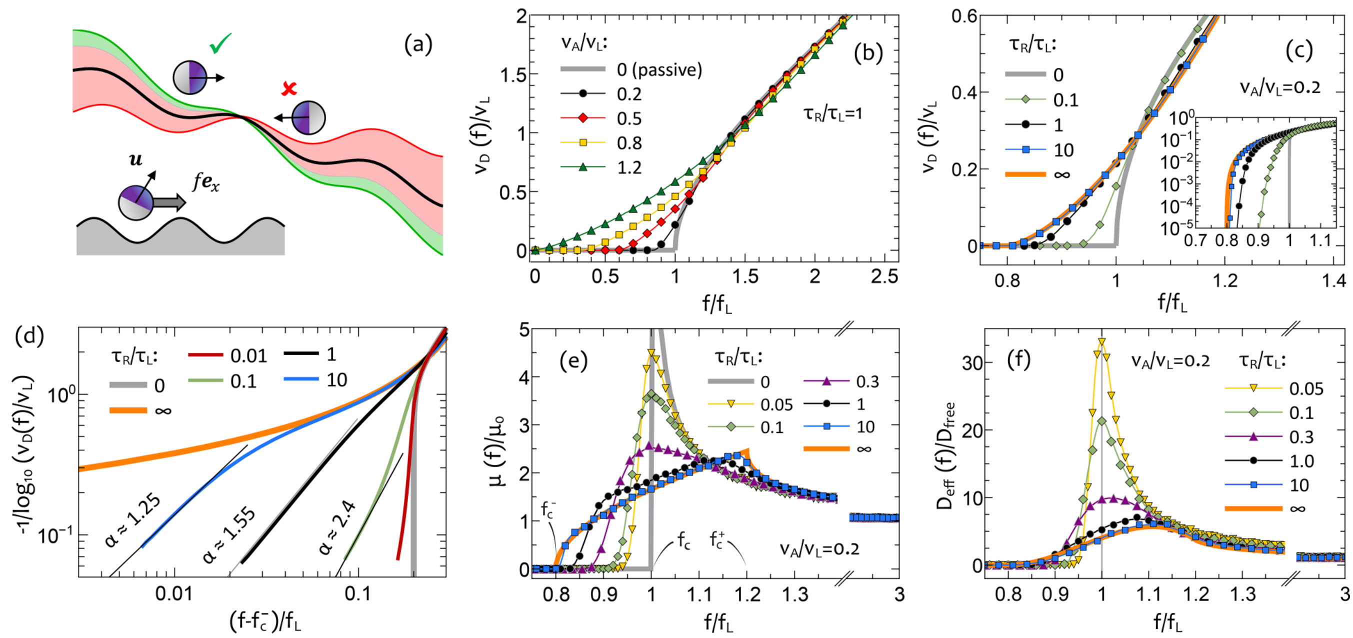

FIG. 1. Panel (a): depinning of an active Janus particle from a corrugated potential landscape and subject to a driving force f (bottom). The problem can be mapped to passive motion in a randomly tilted potential landscape (top) such that the tilt has a constant contribution $-fx$ (black line) which, depending on the orientation $\boldsymbol{u}(t)$, is increased (green line) or decreased (red line) by random, finite amounts. Panels (b),(c): drift velocity $v_{\mathrm{D}}(f)$ of the active particle with (b) fixed orientational persistence time $\tau_{\mathrm{R}} = \tau_{\mathrm{L}}$ but varying propulsion velocity v_{A} and (c) fixed $v_{\mathrm{A}} = 0.2v_{\mathrm{L}}$ but varying τ_{R}. In panel (b), the inset shows the same data as in the main panel on a logarithmic scale. Panel (d): high-precision data for $v_{\mathrm{D}}(f)/v_{\mathrm{L}}$ from the numerical solution of the Fokker-Planck equation, shown on an iterated logarithmic scale and corroborating the superexponential convergence of $v_{\mathrm{D}}(f) \to 0$ as $f \downarrow f_c^-$ [Eq. (6)]. Panels (e),(f): differential mobility $\mu(f) = \mathrm{d}v_{\mathrm{D}}(f)/\mathrm{d}f$ and effective diffusion constant $D_{\mathrm{eff}}(f)$ as functions of the driving force f for fixed $v_{\mathrm{A}} = 0.2v_{\mathrm{L}}$ and varying τ_{R}. All panels: thin lines interpolate between stochastic simulation results (symbols); thick lines are analytic predictions for the limits of the hyper wobbler (gray, $\tau_{\mathrm{R}} \to 0$) and the lazy wobbler (orange, $\tau_{\mathrm{R}} \to \infty$).

As potential we use a corrugated landscape with the prototypical sinusoidal shape [72]: $U(\boldsymbol{r}) = U_{\mathrm{L}}(1 - \cos kx)$ with $x = \boldsymbol{r} \cdot \boldsymbol{e}_x$ and the unit vector $\boldsymbol{e}_x$ pointing perpendicular to the ripples; $2U_{\mathrm{L}}$ is the barrier height, $\lambda = 2\pi/k$ is the period length, and k the corresponding wave number. We fix the direction of the force to $\boldsymbol{f} = f\boldsymbol{e}_x$ ($f \geqslant 0$) and, focusing on the depinning singularity, switch off the translational Brownian noise ($D_0 = 0$), which is known to mask the critical singularity, leading to a rounded rather than a sharp transition [73–75]. This reduces the model to an Adler equation amended by the "active noise" $v_{\mathrm{A}}u_x(t) = v_{\mathrm{A}}\boldsymbol{u}(t) \cdot \boldsymbol{e}_x$:

$$\dot{x}(t) = \mu_0[f - f_{\mathrm{L}} \sin(kx(t))] + v_{\mathrm{A}}u_x(t). \tag{2}$$

The force $f_{\mathrm{L}} = U_{\mathrm{L}}k$, the velocity $v_{\mathrm{L}} = \mu_0 f_{\mathrm{L}}$, and the timescale $\tau_{\mathrm{L}} = \lambda/v_{\mathrm{L}}$ serve as an intrinsic system of independent units. Regimes of different responses are then distinguished by comparing the relative strengths of the external driving f/f_{L} and of the rotational noise $\tau_{\mathrm{R}}/\tau_{\mathrm{L}}$ to unity. For the stochastic simulations, we combined Euler integration of Eq. (2) with a geometric scheme for Eq. (1b) [66] and noise reduction [76]. The drift velocity was calculated from averaging over the driven stationary ensemble as $v_{\mathrm{D}}(f) = \lim_{t\to\infty} \langle x(t) \rangle_f / t$ and the dispersion coefficient followed from the variance $D_{\mathrm{eff}}(f) = \lim_{t\to\infty} \mathrm{Var}[x(t)]_f / 2t$.

The right-hand side of Eq. (2) may also be viewed as originating from a time-dependent tilted potential $U(x) - f_{\mathrm{A}}(t)x$ with $f_{\mathrm{A}}(t) = f + (v_{\mathrm{A}}/\mu_0)u_x(t)$. Its barriers can only be crossed if $u_x(t) > u_{x,\mathrm{c}} = (v_{\mathrm{L}}/v_{\mathrm{A}})(1 - f/f_{\mathrm{L}})$ [Fig. 1(a), green shading], which lets them act as a randomly rocking ratchet, rectifying the *a priori* unbiased self-propelled motion and thus facilitating transport.

We note that the active noise $v_{\mathrm{A}}\boldsymbol{u}(t)$ differs qualitatively from the thermal, white noise $\boldsymbol{\xi}(t)$, both entering Eq. (1a): $v_{\mathrm{A}}\boldsymbol{u}(t)$ is bounded in magnitude, whereas $\boldsymbol{\xi}(t)$ can assume arbitrarily large values. Only in the latter case is the probability of crossing the potential barrier nonzero for any, even small, driving force. Mathematically, the integral $\int_0^t v_{\mathrm{A}}\boldsymbol{u}(s)\,\mathrm{d}s$ is a finite-variation process, unlike the Wiener process $\int_0^t \boldsymbol{\xi}(s)\,\mathrm{d}s$, and thus yields a drift rather than a diffusion term in the Fokker-Planck operator (see [76,77]). Hence the active noise can be interpreted as a random tilting of the potential landscape but not as an intrinsic diffusion.

Depinning transition. Driving passive particles ($v_{\mathrm{A}} = 0$) with $f > f_{\mathrm{L}} =: f_{\mathrm{c}}$, they depin from the confining potential and drift with the velocity [78]

$$v_{\mathrm{D}}^{(\mathrm{p})}(f) = \mu_0\sqrt{f^2 - f_{\mathrm{L}}^2}, \quad f > f_{\mathrm{L}}. \tag{3}$$

Otherwise, $v_{\mathrm{D}}^{(\mathrm{p})}(f) = 0$. Expanding Eq. (3) close to its critical point, $f_{\mathrm{c}} = f_{\mathrm{L}}$, yields a square-root singularity:

$$v_{\mathrm{D}}^{(\mathrm{p})}(f \downarrow f_{\mathrm{c}}) \sim (f - f_{\mathrm{c}})^{\beta}, \quad \beta = 1/2. \tag{4}$$

For self-propelled particles, simulations of Eq. (2) show that the force-velocity relationship $v_{\mathrm{D}}(f)$ deviates progressively stronger from this law upon increasing the propulsion strength v_{A} while fixing the orientational persistence,

$\tau_R = \tau_L$ [Fig. 1(b)]. Conversely, changing τ_R at fixed $v_A = 0.2 v_L$ yields a similar picture [Fig. 1(c)], which remains for other values of τ_R or v_A. Importantly, the ABP with $v_A > 0$ and $\tau_R > 0$ displays a nonzero drift also for $f < f_c$. At first sight, this seems to resemble the rounding of the depinning transition caused by translational Brownian noise [73]. However, we will show that the effect of active propulsion on the transition is entirely different and cannot be mimicked by translational diffusion, $D_0 > 0$. In particular, the self-propelled particle is pinned for $f < f_c^-$ with the shifted threshold $f_c^- = f_L - v_A/\mu_0$ [79].

The existence of an activity-controlled critical force f_c^- is justified by the second observation: upon increasing τ_R from 0 to ∞ at fixed $v_A < v_L$ [Fig. 1(c)], the force-velocity curves vary monotonically between the analytical solutions for the two limiting cases, $\tau_R \to 0$ and $\tau_R \to \infty$, which we shall develop below. Both bounds yield $v_D(f) = 0$ if $f < f_c^-$, which implies a sharp transition for all values of τ_R.

Scaling regimes. We refer to the case of small τ_R as a "hyper wobbler," i.e., an ABP with a rapidly changing orientation such that τ_R is the smallest timescale of the problem, $\tau_R \ll \tau_L$ and $\tau_R \ll \tau_f = \lambda/(\mu_0 f)$. Such an ABP quickly samples all possible orientations before any translation occurs and the active noise $u_x(t)$ is averaged out from Eq. (2). Thus self-propulsion is inefficient for the hyper wobbler, leading to creep for $f_c^- < f < f_c$ with a strongly suppressed drift. Letting $\tau_R \to 0$, Eq. (3) holds again and the scaling exponent $\beta = 1/2$ is obeyed.

The opposite regime describes a "lazy wobbler" ($\tau_R \gg \tau_L, \tau_f$), which changes its orientation slowly. The trajectories $x(t)$ can be thought of as a random walk composed of a sequence of long independent segments $i = 1, 2, \ldots$ with fixed orientations $\boldsymbol{u}_i$ isotropically distributed and randomly changing at random times with rate τ_R^{-1}; equivalently, we specify polar angles ϑ_i such that $u_{x,i} = \cos\vartheta_i$. The regime is identified with the standard model for RTPs with switching rate τ_R^{-1} [70,71]. Pictorially, transport is fastest if the orientation is fixed in the direction of the driving force ($\vartheta = 0$), whereas the opposite direction ($\vartheta = \pi$) is the most inefficient situation [Fig. 1(a)]. The increased persistence leads to a well-developed drift for $f_c^- < f < f_c$. For large $\tau_R < \infty$, different angles ϑ_i are sampled over time and $v_D(f)$ is not simply a shifted version of the curve $v_D^{(p)}(f)$. Instead, $v_D(f)$ appears smoother near the transition at $f = f_c^-$, which is apparent from the exact solution $v_D^{(\infty)}(f)$ for $\tau_R \to \infty$ [cf. Eq. (8)] exhibiting a larger critical exponent:

$$v_D^{(\infty)}(f \downarrow f_c^-) \sim (f - f_c^-)^{\beta'}, \quad \beta' = 3/2\,. \tag{5}$$

Creep regime. How are the critical laws (4) and (5) connected upon changing τ_R? Do the force threshold and the scaling exponent vary continuously? Since the stochastic simulation data [Fig. 1(c)] are not sufficiently conclusive to answer these questions, we have obtained precise numerical solutions of the corresponding Fokker-Planck equation [Fig. 1(d)], allowing us to follow $v_D(f)/v_L$ down to 10^{-15} [76]. These semianalytical results suggest a creep regime with superexponential rather than power-law behavior:

$$v_D(f) \simeq v_L \exp[-b(f - f_c^-)^{-\alpha}], \quad f \downarrow f_c^-. \tag{6}$$

The coefficients $\alpha > 1$ and $b > 0$ depend on τ_R and we found that α decreases as τ_R is increased. The form of Eq. (6) is in line with predictions from related discrete-time models [80,81] and it is rooted in a very slow initial increase of the probability that the particle slips along $\boldsymbol{e}_x$ by one period length upon increasing $f > f_c^-$. (This probability is zero for $f < f_c^-$.) For $\tau_R \gg \tau_L$ and upon increasing f further, the behavior (6) crosses over to closely follow the lazy-wobbler solution, $v_D(f) \approx v_D^{(\infty)}(f)$. We conclude that $v_D(f) > 0$ for $f > f_c^-$, i.e., the critical point is the same for all $\tau_R > 0$.

Differential mobility. The differential mobility $\mu(f) = \mathrm{d}v_D(f)/\mathrm{d}f$ is an alternative measure of the transport and more sensitive to singular behavior [Fig. 1(e)]. For $0 < \tau_R < \infty$, we have calculated $\mu(f)$ from the numerical results for $v_D(f)$ and it is readily obtained analytically for the limiting cases [Eqs. (3) and (8)]. In any situation, the potential landscape becomes irrelevant for sufficiently strong driving, $\mu(f \to \infty) = \mu_0$. For the hyper wobbler ($\tau_R \to 0$), the mobility diverges at the corresponding critical force, $\mu_p(f \downarrow f_c) \sim (f - f_c)^{-1/2}$, whereas it vanishes as $\mu_\infty(f \downarrow f_c^-) \sim (f - f_c^-)^{1/2}$ for the lazy wobbler. In addition, $\mu_\infty(f)$ remains finite but exhibits a cusp at the force $f_c^+ = f_L + v_A/\mu_0$, pinpointing the presence of a second singular point, at which $\mu_\infty(f)$ is maximal. In between these limiting cases, the mobility has a maximum that, upon varying τ_R, interpolates in peak height and position between the divergence at $f = f_c$ ($\tau_R \ll \tau_L$) and the cusp at $f = f_c^+$ ($\tau_R \gg \tau_L$). Concomitantly, the left flank of the peak moves from $f = f_c$ to f_c^-, broadening the peak.

Activity-induced giant diffusion. For passive depinning, the differential mobility is a good proxy of the dispersion coefficient, $D_{\mathrm{eff}}(f) \propto \mu(f)$, which restores a linear response relation [82]. For ABPs with small τ_R, the curves of $D_{\mathrm{eff}}(f)$ and $\mu(f)$ are strikingly similar [Figs. 1(e) and 1(f)]; in particular, $D_{\mathrm{eff}}(f)/D_{\mathrm{free}}$ shows a peak near the transition ($f \approx f_c$), which grows in height without bounds as $\tau_R \to 0$; $D_{\mathrm{free}} = v_A^2 \tau_R/3$ is the effective diffusion of the free ABP. Such giant diffusion was studied for passive particles [83–85] and has been seen in experiments [27,86]; similar behavior was found for circle swimmers subject to gravity [26].

For lazy wobblers (large τ_R), the corrugated potential induces a different kind of enhanced dispersion. In this regime, the data for $D_{\mathrm{eff}}(f)/D_{\mathrm{free}}$ depend only weakly on τ_R and closely follow the exact result for $D_{\mathrm{eff}}(f)$ [Fig. 1(f), orange line]. The latter follows from again invoking the random walk picture of uncorrelated velocities $v_D(f; \vartheta_i)$ changing at a "collision rate" τ_R^{-1}; see Eqs. (S22) and (S25) of [76]. The curve shows a maximum $D_{\max} = D_{\mathrm{eff}}(f_{\max})$ near $f_{\max} \approx (f_c + f_c^+)/2$. Expanding for $v_A \ll v_L$ yields

$$D_{\max} \simeq (9D_{\mathrm{free}}/8)(v_L/v_A + 3/5), \tag{7}$$

which predicts an 6.3-fold enhancement of $D_{\mathrm{eff}}(f)$ over D_{free} for $v_A = 0.2 v_L$, as is observed in the data for $\tau_R = 10\tau_L$ near $f \approx 1.1 f_L$ [Fig. 1(f)]. We anticipate an arbitrarily large enhancement of the dispersion, $D_{\max}/D_{\mathrm{free}} \sim 1/v_A$, for weakly self-propelled particles with $\tau_R \gtrsim \tau_L$.

Analytical theory. Before developing the theory for self-propelled particles, we briefly recall the passive case. For $v_A = 0$, the particle motion is governed by the dynamic system $\dot{x} = g(x, f)$ with $g(x, f) = \mu_0(f - f_L \sin kx)$, which exhibits a saddle-node bifurcation [87]. Two equilibria $x_*^\pm \in$

$[0, \lambda)$, obeying $g(x_*, f) = 0$, exist for $f < f_c$ and disappear at the critical point $f_c = f_L$, which fulfills the additional requirement $\partial_x g(x_*, f_c) = 0$. Thus the particle is pinned for $f < f_L$ and remains immobile, $v_D^{(p)}(f) = 0$. For $f > f_L$, the particle slides with $v_D^{(p)}(f) = \lambda/\tau_1(f)$, where $\tau_1(f) = \int_0^\lambda g(x, f)^{-1}\,dx$ is the time it takes to travel one wavelength. Evaluating the integral for the sinusoidal potential yields $v_D^{(p)}(f)$ in Eq. (3), which admits for the scaling form $v_D^{(p)}(f) = v_L s(f/f_L)$ with the rescaled force $y = f/f_L$ and the scaling function $s(y) = \sqrt{y^2 - 1}$ for $|y| > 1$ and $s(y) = 0$ otherwise.

For an ABP with fixed orientation $\boldsymbol{u}$, the active noise term in Eq. (2) can be absorbed in the shifted driving force $f_A(\vartheta) = f + (v_A/\mu_0)\cos\vartheta$, where $u_x = \cos\vartheta$. With this, the dynamic system reads again $\dot{x} = g(x, f_A(\vartheta))$ and it follows that the velocity-force relationship of an ABP with prescribed orientation ϑ has the same functional form: $v_D(f;\vartheta) = v_L s(f_A(\vartheta)/f_L)$. Merely the condition $|f_A(\vartheta)| > f_c$ implies a shift of the critical point from $f_c = f_L$ to $f_L - (v_A/\mu_0)\cos\vartheta$. The latter expression depends on ϑ and varies between the values $f_c^\pm = f_L \pm v_A/\mu_0$. In particular, $v_D(f;\vartheta) = 0$ for $f \leqslant f_c^-$ irrespective of ϑ.

For lazy wobblers (large τ_R), we employ the RTP model where $x(t)$ is a random walk with random orientations $\boldsymbol{u}_i$ and thus velocities $v_D(f;\vartheta_i)$. At long times, this implies a uniform average over the orientation, $\langle\cdot\rangle_{\boldsymbol{u}} := (4\pi)^{-1}\int \cdot\, \sin\vartheta\, d\vartheta\, d\varphi$. For the mean drift of the lazy wobbler, it follows $v_D^{(\infty)}(f) = \lim_{t\to\infty}\langle x(t)/t\rangle_f = \langle v_D(f;\vartheta)\rangle_{\boldsymbol{u}}$ and, specifically [76],

$$v_D^{(\infty)}(f) = \frac{v_L^2}{2v_A}[w_+(f/f_L) - w_-(f/f_L)], \tag{8}$$

introducing additional scaling functions $w_\pm(y) = w(y \pm v_A/v_L)$ with $w(z) = \int_0^z s(y)dy$. The integral evaluates to $w(z) = \{zs(z) - \ln[z + s(z)]\}/2$ if $z > 1$; otherwise, $w(z) = 0$; in particular, $w_\pm(f/f_L) = 0$ for $f \leqslant f_c^\mp$. The passive limit [Eq. (3)] is recovered as $v_A \to 0$; in this limit, the two singular points $f_c^\pm$ converge to $f_c = f_L$. Due to $w'(z) = s(z)$, the critical exponent β increases by 1, turning the square-root singularity [Eq. (4)] into Eq. (5).

The argument applies similarly for rotational motion in a plane, noting that u_x is distributed differently in this case. Analysis of the leading asymptotic behavior upon $\varepsilon := (f - f_c^-)/f_L \downarrow 0$ yields for $d = 2, 3$ dimensions [76]

$$v_D^{(\infty)}(\varepsilon \downarrow 0) \simeq \frac{\sqrt{d-1}}{d}\, v_L^{1/2+\beta'}\, v_A^{1/2-\beta'}\, \varepsilon^{\beta'}, \quad \beta' = d/2. \tag{9}$$

Intuitively, the behavior of $v_D^{(\infty)}(f)$ near $f \approx f_c^-$ may be understood from the random tilts of the potential landscape [Fig. 1(a)]: in an ensemble of particles, only those with orientations pointing sufficiently close towards the direction of the force contribute to the transport: $u_x > u_{x,c} = 1 - \varepsilon v_L/v_A$ so that $v_D(f;\vartheta) > 0$. Near the transition, $u_{x,c} \to 1$ and the square-root behavior $v_D(f;\vartheta) \sim (u_x - u_{x,c})^{1/2}$ is weighted with the distribution of u_x close to 1: the latter is flat for $d = 3$, but divergent $\sim (1 - u_x)^{-1/2}$ for $d = 2$. Both factors combine into $\sim (1 - u_{x,c})^{d/2}$ after integration and hence $\beta' = d/2$. Transport near criticality is thus faster for $d = 2$ than for $d = 3$ (Fig. S2 in [76]).

Conclusions. We have shown analytically and numerically that activity alters the depinning transition: a sharp transition is preserved in the presence of self-propulsion, yet with the threshold force shifted from its value f_c for passive particles to $f_c^- < f_c$; the threshold depends on the propulsion strength v_A but not on the orientational persistence time τ_R. However, the approach to the transition from above depends on τ_R and on the dimension d of rotational motion: it obeys different power laws for the limits of the hyper and lazy wobbler with exponents $\beta = 1/2$ (small τ_R) and $\beta' = d/2$ (large τ_R), respectively. In between, there is a creep regime where $v_D(f)$ vanishes superexponentially fast, contrasting from the scenario of a τ_R-dependent exponent. For the lazy wobbler, another singular point f_c^+ emerges as the mirror image of f_c^- relative to f_c; at f_c^+, the differential mobility $\mu(f)$ is maximum. Eventually, the dispersion coefficient shows a giant enhancement whose scaling and position depend on τ_R. It would be interesting to connect our findings with a recent formalism for activity-assisted escape valid for small, nonzero D_0 [59]. Regarding a perturbative treatment of the passive case with τ_R as the small parameter (e.g., Refs. [77,88]), it appears unlikely that the discontinuous changes of the phenomenology can be captured. Our work suggests that probing nonlinear responses [35–37] can stimulate a similar debate for arrested active matter [89–91].

The described transition scenario is in marked contrast to the rounding of the transition due to translational thermal noise [73–75] or in an active bath [92]. We have attributed the changes to the bounded magnitude of the active noise, which has the effect of a random tilting of the confining potential. We anticipate that analogous findings apply to other dynamic systems with bounded noise near a saddle-node bifurcation [80,81].

Our predictions appear amenable to experimental tests, e.g., using active colloidal particles driven by external fields (e.g., gravitational [29,93,94] or magnetic [25,33]) over a periodic landscape [48,51,68] and potentially for the chemotaxis of bacteria crawling on structured substrates [61,62]. Experiments on active colloidal monolayers may give insight into the activity-induced depinning of collective variables and our study is relevant for the melting transition of active colloidal crystals [95].

Acknowledgments. We thank A. Pikovsky for helpful discussions. Financial support by Deutsche Forschungsgemeinschaft (DFG, German Research Foundation) under Germany's Excellence Strategy—MATH+: The Berlin Mathematics Research Center (EXC-2046/1)—Project No. 390685689 (Subprojects No. AA1-18 and No. EF4-10) and further under Project No. 523950429 is gratefully acknowledged.

[1] D. S. Fisher, Collective transport in random media: From superconductors to earthquakes, Phys. Rep. **301**, 113 (1998).

[2] S. Brazovskii and T. Nattermann, Pinning and sliding of driven elastic systems: From domain walls to charge density waves, Adv. Phys. **53**, 177 (2004).

[3] C. Reichhardt and C. J. O. Reichhardt, Depinning and nonequilibrium dynamic phases of particle assemblies driven over random and ordered substrates: a review, Rep. Prog. Phys. **80**, 026501 (2017).
[4] F. Haudin, R. G. Elípas, R. G. Rojas, U. Bortolozzo, M. G. Clerc, and S. Residori, Driven front propagation in 1D spatially periodic media, Phys. Rev. Lett. **103**, 128003 (2009).
[5] A. Carpio and L. L. Bonilla, Wave front depinning transition in discrete one-dimensional reaction-diffusion systems, Phys. Rev. Lett. **86**, 6034 (2001).
[6] F. Martinez-Pedrero, P. Tierno, T. H. Johansen, and A. V. Straube, Regulating wave front dynamics from the strongly discrete to the continuum limit in magnetically driven colloidal systems, Sci. Rep. **6**, 19932 (2016).
[7] Y. Jiang, Y. Sun, J. W. Drelich, and C.-H. Choi, Topography-dependent effective contact line in droplet depinning, Phys. Rev. Lett. **125**, 184502 (2020).
[8] K. J. A. Franke, B. Van de Wiele, Y. Shirahata, S. J. Hämäläinen, T. Taniyama, and S. van Dijken, Reversible electric-field-driven magnetic domain-wall motion, Phys. Rev. X **5**, 011010 (2015).
[9] S. Woo, T. Delaney, and G. S. D. Beach, Magnetic domain wall depinning assisted by spin wave bursts, Nat. Phys. **13**, 448 (2017).
[10] N. Bauer, S. M. Neumayer, P. Maksymovych, and M. O. Lavrentovich, Structures and velocities of noisy ferroelectric domain walls, Phys. Rev. Mater. **6**, 124401 (2022).
[11] G. Blatter, M. V. Feigel'man, V. B. Geshkenbein, A. I. Larkin, and V. M. Vinokur, Vortices in high-temperature superconductors, Rev. Mod. Phys. **66**, 1125 (1994).
[12] M. Buchacek, R. Willa, V. B. Geshkenbein, and G. Blatter, Strong pinning theory of thermal vortex creep in type-II superconductors, Phys. Rev. B **100**, 014501 (2019).
[13] Y. Fily, E. Olive, N. Di Scala, and J. C. Soret, Critical behavior of plastic depinning of vortex lattices in two dimensions: Molecular dynamics simulations, Phys. Rev. B **82**, 134519 (2010).
[14] S.-Z. Lin, C. Reichhardt, C. D. Batista, and A. Saxena, Particle model for skyrmions in metallic chiral magnets: Dynamics, pinning, and creep, Phys. Rev. B **87**, 214419 (2013).
[15] A. Vanossi, N. Manini, M. Urbakh, S. Zapperi, and E. Tosatti, *Colloquium*: Modeling friction: From nanoscale to mesoscale, Rev. Mod. Phys. **85**, 529 (2013).
[16] A. Bylinskii, D. Gangloff, and V. Vuletić, Tuning friction atom-by-atom in an ion-crystal simulator, Science **348**, 1115 (2015).
[17] A. Vanossi, C. Bechinger, and M. Urbakh, Structural lubricity in soft and hard matter systems, Nat. Commun. **11**, 4657 (2020).
[18] T. Brazda, A. Silva, N. Manini, A. Vanossi, R. Guerra, E. Tosatti, and C. Bechinger, Experimental observation of the Aubry transition in two-dimensional colloidal monolayers, Phys. Rev. X **8**, 011050 (2018).
[19] O. Hod, E. Meyer, Q. Zheng, and M. Urbakh, Structural superlubricity and ultralow friction across the length scales, Nature (London) **563**, 485 (2018).
[20] M. P. N. Juniper, A. V. Straube, R. Besseling, D. G. A. L. Aarts, and R. P. A. Dullens, Microscopic dynamics of synchronization in driven colloids, Nat. Commun. **6**, 7187 (2015).
[21] P. T. Korda, M. B. Taylor, and D. G. Grier, Kinetically locked-in colloidal transport in an array of optical tweezers, Phys. Rev. Lett. **89**, 128301 (2002).
[22] M. Balvin, E. Sohn, T. Iracki, G. Drazer, and J. Frechette, Directional locking and the role of irreversible interactions in deterministic hydrodynamics separations in microfluidic devices, Phys. Rev. Lett. **103**, 078301 (2009).
[23] M. P. N. Juniper, U. Zimmermann, A. V. Straube, R. Besseling, D. G. A. L. Aarts, H. Löwen, and R. P. A. Dullens, Dynamic mode locking in a driven colloidal system: experiments and theory, New J. Phys. **19**, 013010 (2017).
[24] X. Cao, E. Panizon, A. Vanossi, N. Manini, and C. Bechinger, Orientational and directional locking of colloidal clusters driven across periodic surfaces, Nat. Phys. **15**, 776 (2019).
[25] R. L. Stoop, A. V. Straube, T. H. Johansen, and P. Tierno, Collective directional locking of colloidal monolayers on a periodic substrate, Phys. Rev. Lett. **124**, 058002 (2020).
[26] O. Chepizhko and T. Franosch, Resonant diffusion of a gravitactic circle swimmer, Phys. Rev. Lett. **129**, 228003 (2022).
[27] M. Evstigneev, O. Zvyagolskaya, S. Bleil, R. Eichhorn, C. Bechinger, and P. Reimann, Diffusion of colloidal particles in a tilted periodic potential: Theory versus experiment, Phys. Rev. E **77**, 041107 (2008).
[28] A. V. Straube and P. Tierno, Synchronous vs. asynchronous transport of a paramagnetic particle in a modulated ratchet potential, Europhys. Lett. **103**, 28001 (2013).
[29] X.-g. Ma, P.-Y. Lai, B. J. Ackerson, and P. Tong, Colloidal transport and diffusion over a tilted periodic potential: Dynamics of individual particles, Soft Matter **11**, 1182 (2015).
[30] M. P. N. Juniper, A. V. Straube, D. G. A. L. Aarts, and R. P. A. Dullens, Colloidal particles driven across periodic optical-potential-energy landscapes, Phys. Rev. E **93**, 012608 (2016).
[31] A. Pertsinidis and X. S. Ling, Statics and dynamics of 2D colloidal crystals in a random pinning potential, Phys. Rev. Lett. **100**, 028303 (2008).
[32] T. Bohlein, J. Mikhael, and C. Bechinger, Observation of kinks and antikinks in colloidal monolayers driven across ordered surfaces, Nat. Mater. **11**, 126 (2012).
[33] P. Tierno, Depinning and collective dynamics of magnetically driven colloidal monolayers, Phys. Rev. Lett. **109**, 198304 (2012).
[34] M. Hülsberg and S. H. L. Klapp, Depinning dynamics of confined colloidal dispersions under oscillatory shear, Phys. Rev. E **107**, 014603 (2023).
[35] D. Winter and J. Horbach, Nonlinear active micro-rheology in a glass-forming soft-sphere mixture, J. Chem. Phys. **138**, 12A512 (2013).
[36] N. Şenbil, M. Gruber, C. Zhang, M. Fuchs, and F. Scheffold, Observation of strongly heterogeneous dynamics at the depinning transition in a colloidal glass, Phys. Rev. Lett. **122**, 108002 (2019).
[37] M. Gruber, A. M. Puertas, and M. Fuchs, Critical force in active microrheology, Phys. Rev. E **101**, 012612 (2020).
[38] P. Romanczuk, M. Bär, W. Ebeling, B. Lindner, and L. Schimansky-Geier, Active Brownian particles, Eur. Phys. J. Spec. Top. **202**, 1 (2012).
[39] I. S. Aranson, Active colloids, Phys. Usp. **56**, 79 (2013).

[40] J. Elgeti, R. G. Winkler, and G. Gompper, Physics of microswimmers—single particle motion and collective behavior: A review, Rep. Prog. Phys. **78**, 056601 (2015).

[41] C. Bechinger, R. Di Leonardo, H. Löwen, C. Reichhardt, G. Volpe, and G. Volpe, Active particles in complex and crowded environments, Rev. Mod. Phys. **88**, 045006 (2016).

[42] A. Zöttl and H. Stark, Emergent behavior in active colloids, J. Phys.: Condens. Matter **28**, 253001 (2016).

[43] B. J. Nelson, I. K. Kaliakatsos, and J. J. Abbott, Microrobots for minimally invasive medicine, Annu. Rev. Biomed. Eng. **12**, 55 (2010).

[44] S. Palagi and P. Fischer, Bioinspired microrobots, Nat. Rev. Mater. **3**, 113 (2018).

[45] Y. Alapan, O. Yasa, O. Schauer, J. Giltinan, A. F. Tabak, V. Sourjik, and M. Sitti, Soft erythrocyte-based bacterial microswimmers for cargo delivery, Sci. Robot. **3**, eaar4423 (2018).

[46] Z. Xiao, M. Wei, and W. Wang, A review of micromotors in confinements: Pores, channels, grooves, steps, interfaces, chains, and swimming in the bulk, ACS Appl. Mater. Interfaces **11**, 6667 (2019).

[47] M. R. Shaebani, A. Wysocki, R. G. Winkler, G. Gompper, and H. Rieger, Computational models for active matter, Nat. Rev. Phys. **2**, 181 (2020).

[48] U. Choudhury, A. V. Straube, P. Fischer, J. G. Gibbs, and F. Höfling, Active colloidal propulsion over a crystalline surface, New J. Phys. **19**, 125010 (2017).

[49] A. V. Straube, J. M. Pagès, P. Tierno, J. Ignés-Mullol, and F. Sagués, Collective dynamics and conformal ordering in electrophoretically driven nematic colloids, Phys. Rev. Res. **1**, 022008 (2019).

[50] A. Ryabov and M. Tasinkevych, Mechanochemical active ratchet, Sci. Rep. **13**, 20572 (2023).

[51] Y. Wen, Z. Li, H. Wang, J. Zheng, J. Tang, P.-Y. Lai, X. Xu, and P. Tong, Activity-assisted barrier crossing of self-propelled colloids over parallel microgrooves, Phys. Rev. E **107**, L032601 (2023).

[52] M. Su and B. Lindner, Active Brownian particles in a biased periodic potential, Eur. Phys. J. E **46**, 22 (2023).

[53] P. Bag, S. Nayak, T. Debnath, and P. K. Ghosh, Directed autonomous motion and chiral separation of self-propelled Janus particles in convection roll arrays, J. Phys. Chem. Lett. **13**, 11413 (2022).

[54] P. K. Ghosh, P. Hänggi, F. Marchesoni, and F. Nori, Giant negative mobility of Janus particles in a corrugated channel, Phys. Rev. E **89**, 062115 (2014).

[55] P. Rizkallah, A. Sarracino, O. Bénichou, and P. Illien, Absolute negative mobility of an active tracer in a crowded environment, Phys. Rev. Lett. **130**, 218201 (2023).

[56] S. Pattanayak, R. Das, M. Kumar, and S. Mishra, Enhanced dynamics of active Brownian particles in periodic obstacle arrays and corrugated channels, Eur. Phys. J. E **42**, 62 (2019).

[57] A. Geiseler, P. Hänggi, and G. Schmid, Kramers escape of a self-propelled particle, Eur. Phys. J. B **89**, 175 (2016).

[58] A. Sharma, R. Wittmann, and J. M. Brader, Escape rate of active particles in the effective equilibrium approach, Phys. Rev. E **95**, 012115 (2017).

[59] E. Woillez, Y. Zhao, Y. Kafri, V. Lecomte, and J. Tailleur, Activated escape of a self-propelled particle from a metastable state, Phys. Rev. Lett. **122**, 258001 (2019).

[60] A. Militaru, M. Innerbichler, M. Frimmer, F. Tebbenjohanns, L. Novotny, and C. Dellago, Escape dynamics of active particles in multistable potentials, Nat. Commun. **12**, 2446 (2021).

[61] G. Amselem, M. Theves, A. Bae, E. Bodenschatz, and C. Beta, A stochastic description of Dictyostelium chemotaxis, PLoS ONE **7**, e37213 (2012).

[62] L. Rußbach, M. Ecke, J. O. Rädler, C. Leu, and G. Gerisch, Cells responding to chemoattractant on a structured substrate, Biophys. J. **121**, 2557 (2022).

[63] C. Reichhardt and C. J. O. Reichhardt, Clogging and depinning of ballistic active matter systems in disordered media, Phys. Rev. E **97**, 052613 (2018).

[64] S. Nayak, S. Das, P. Bag, T. Debnath, and P. K. Ghosh, Driven transport of active particles through arrays of symmetric obstacles, J. Chem. Phys. **159**, 164109 (2023).

[65] S. Leitmann, F. Höfling, and T. Franosch, Tube concept for entangled stiff fibers predicts their dynamics in space and time, Phys. Rev. Lett. **117**, 097801 (2016); Dynamically crowded solutions of infinitely thin Brownian needles, Phys. Rev. E **96**, 012118 (2017).

[66] F. Höfling and A. V. Straube, Langevin equations and a geometric integration scheme for the overdamped limit of homogeneous rotational Brownian motion, arXiv:2403.04501 [cond-mat.stat-mech].

[67] M. Enculescu and H. Stark, Active colloidal suspensions exhibit polar order under gravity, Phys. Rev. Lett. **107**, 058301 (2011).

[68] J. G. Gibbs, Shape- and material-dependent self-propulsion of photocatalytic active colloids, interfacial effects, and dynamic interparticle interactions, Langmuir **36**, 6938 (2020).

[69] V. Carrasco-Fadanelli and I. Buttinoni, Sedimentation and levitation of catalytic active colloids, Phys. Rev. Res. **5**, L012018 (2023).

[70] M. J. Schnitzer, Theory of continuum random walks and application to chemotaxis, Phys. Rev. E **48**, 2553 (1993).

[71] A. P. Solon, M. E. Cates, and J. Tailleur, Active Brownian particles and run-and-tumble particles: A comparative study, Eur. Phys. J. Spec. Top. **224**, 1231 (2015).

[72] A. V. Straube and F. Höfling, Memory effects in colloidal motion under confinement and driving, J. Phys. A: Math. Theor. **57**, 295003 (2024).

[73] R. L. Stratonovich, *Topics in the Theory of Random Noise* (Gordon and Breach, New York, 1967), Vol. II.

[74] A. A. Middleton, Thermal rounding of the charge-density-wave depinning transition, Phys. Rev. B **45**, 9465 (1992).

[75] A. B. Kolton and E. A. Jagla, Thermally rounded depinning of an elastic interface on a washboard potential, Phys. Rev. E **102**, 052120 (2020).

[76] See Supplemental Material at http://link.aps.org/supplemental/10.1103/PhysRevE.110.L062601 for a description of the numerics and for intermediate steps of the mathematical derivations.

[77] G. Szamel, Self-propelled particle in an external potential: Existence of an effective temperature, Phys. Rev. E **90**, 012111 (2014).

[78] S. Strogatz, *Nonlinear Dynamics and Chaos*, 2nd ed. (CRC Press, Boca Raton, 2019).

[79] For fast active motion, $v_{\mathrm{A}} \geqslant v_{\mathrm{L}}$, the particle depins for any $f > 0$; we exclude this trivial situation here.

[80] G. Olicón Méndez, Critical behaviour of random diffeomorphisms: Quasi-stationary measures and escape times, Ph.D. thesis, Imperial College London, 2020.

[81] V. Chigarev, A. Kazakov, and A. Pikovsky, Attractor–repeller collision and the heterodimensional dynamics, Chaos **33**, 063113 (2023).

[82] G. Costantini and F. Marchesoni, Threshold diffusion in a tilted washboard potential, Europhys. Lett. **48**, 491 (1999).

[83] P. Reimann, C. Van den Broeck, H. Linke, P. Hänggi, J. M. Rubi, and A. Pérez-Madrid, Giant acceleration of free diffusion by use of tilted periodic potentials, Phys. Rev. Lett. **87**, 010602 (2001); Diffusion in tilted periodic potentials: Enhancement, universality, and scaling, Phys. Rev. E **65**, 031104 (2002).

[84] N. J. López-Alamilla, M. W. Jack, and K. J. Challis, Enhanced diffusion and the eigenvalue band structure of Brownian motion in tilted periodic potentials, Phys. Rev. E **102**, 042405 (2020).

[85] B. Lindner and I. M. Sokolov, Giant diffusion of underdamped particles in a biased periodic potential, Phys. Rev. E **93**, 042106 (2016).

[86] R. L. Stoop, A. V. Straube, and P. Tierno, Enhancing nanoparticle diffusion on a unidirectional domain wall magnetic ratchet, Nano Lett. **19**, 433 (2019).

[87] S. H. Strogatz, *Nonlinear Dynamics and Chaos: With Applications to Physics, Biology, Chemistry, and Engineering* (Addison-Wesley, Reading, MA, 1994).

[88] É. Fodor, C. Nardini, M. E. Cates, J. Tailleur, P. Visco, and F. van Wijland, How far from equilibrium is active matter? Phys. Rev. Lett. **117**, 038103 (2016).

[89] K. Paul, A. Mutneja, S. K. Nandi, and S. Karmakar, Dynamical heterogeneity in active glasses is inherently different from its equilibrium behavior, Proc. Natl. Acad. Sci. USA **120**, e2217073120 (2023).

[90] V. E. Debets and L. M. C. Janssen, Active glassy dynamics is unaffected by the microscopic details of self-propulsion, J. Chem. Phys. **157**, 224902 (2022); L. M. C. Janssen, Active glasses, J. Phys.: Condens. Matter **31**, 503002 (2019).

[91] N. Klongvessa, F. Ginot, C. Ybert, C. Cottin-Bizonne, and M. Leocmach, Active glass: Ergodicity breaking dramatically affects response to self-propulsion, Phys. Rev. Lett. **123**, 248004 (2019).

[92] A. Gopal, É. Roldán, and S. Ruffo, Energetics of critical oscillators in active bacterial baths, J. Phys. A: Math. Theor. **54**, 164001 (2021).

[93] J. Palacci, C. Cottin-Bizonne, C. Ybert, and L. Bocquet, Sedimentation and effective temperature of active colloidal suspensions, Phys. Rev. Lett. **105**, 088304 (2010).

[94] A. L. Thorneywork, J. L. Abbott, D. G. A. L. Aarts, and R. P. A. Dullens, Two-dimensional melting of colloidal hard spheres, Phys. Rev. Lett. **118**, 158001 (2017).

[95] H. Massana-Cid, C. Maggi, N. Gnan, G. Frangipane, and R. Di Leonardo, Multiple temperatures and melting of a colloidal active crystal, Nat. Commun. **15**, 6574 (2024).